A Journal of the Gesellschaft Deutscher Chemiker
Angewandte Chemie
GDCh
International Edition
www.angewandte.org

Accepted Article

Title: Directional Ring Translocation in a pH- and Redox-Driven Tristable [2]Rotaxane

Authors: Leonardo Andreoni, Jessica Groppi, Özlem Seven, Massimo Baroncini, Alberto Credi, and Serena Silvi

To be cited as: *Angew. Chem. Int. Ed.* **2024**, e202414609

Link to VoR: https://doi.org/10.1002/anie.202414609

WILEY-VCH

10.1002/anie.202414609

RESEARCH ARTICLE

Directional Ring Translocation in a pH- and Redox-Driven Tristable [2]Rotaxane

Leonardo Andreoni,[a,b] Jessica Groppi,*[b,c] Özlem Seven,[b,c] Massimo Baroncini,[b,d] Alberto Credi,[a,b] and Serena Silvi*[b,e]

[a] Dr. Leonardo Andreoni, Prof. Alberto Credi
Dipartimento di Chimica Industriale "Toso Montanari", Università di Bologna,
viale del Risorgimento 4, 40136 Bologna, Italy.

[b] Dr. Leonardo Andreoni, Dr. Jessica Groppi, Dr. Özlem Seven, Prof. Massimo Baroncini, Prof. Alberto Credi, Prof. Serena Silvi
CLAN-Center for Light Activated Nanostructures, Institute ISOF-CNR,
via Gobetti 101, 40129 Bologna, Italy.
Email: serena.silvi@unibo.it, jessica.groppi@isof.cnr.it

[c] Dr. Jessica Groppi, Dr. Özlem Seven
Institute for Organic Synthesis and Photoreactivity (ISOF), National Research Council of Italy (CNR),
Via P. Gobetti 101, 40129 Bologna, Italy.

[d] Prof. Massimo Baroncini,
Dipartimento di Scienze e Tecnologie Agro-alimentari, Università di Bologna,
viale Fanin 44, 40127 Bologna, Italy.

[e] Prof. Serena Silvi
Dipartimento di Chimica "G. Ciamician", Università di Bologna,
via Selmi 2, 40126 Bologna, Italy.

Supporting information for this article is given via a link at the end of the document.

Abstract: We describe the synthesis and characterization of a [2]rotaxane comprising a dibenzo-24-crown-8 (DB24C8) macrocyclic component and a thread containing three recognition sites: ammonium (AmH^+), bipyridinium (Bpy^{2+}) and triazolium (Trz^+). AmH^+ and Bpy^{2+} are responsive to fully orthogonal stimuli, pH and electrochemical, which allows to precisely control the directional translation of the macrocycle along the axle. A better understanding of the processes driving the operation of the system was obtained thanks to an in-depth thermodynamic characterization. Orthogonal stimuli responsive tristable rotaxanes represent the starting point for the creation of linear motors and the development of molecular logic gates.

Introduction

Rotaxanes are an extensively explored class of mechanically interlocked molecules (MIMs),[1] with particular significance in the field of molecular machines and motors.[2] The minimal system is represented by a [2]rotaxane, composed of an axle-like molecule surrounded by a macrocycle, which cannot dethread by virtue of the presence of bulky units at the extremities of the axle.[3] The presence of complementary recognition sites on the axle and macrocyclic components is generally exploited to template the formation of the interlocked structure and to impart functionality to the system. One can classify rotaxanes according to the number of molecular components and of the interaction sites present on the axle, generally referred to as "stations".[4]

Beside the synthetic challenge presented by the construction of such elaborate structures, equally demanding and stimulating is the design of rotaxane-based functional systems. Indeed two-station (or bistable) [2]rotaxanes constitute the minimal prototype for the realization of linear molecular machines - namely, molecular shuttles - wherein one of the components, e.g., the macrocycle, moves relative to the other (the axle) in a precise and controlled way as a consequence of an external stimulus. In this context, the key requirement is the insertion of a proper recognition site on the axle, since the translation of the ring is achieved by modulation of its relative affinity for the stations.[3, 5] These controlled movements can have interesting implications not only for molecular machinery, but also for the realization of molecular logic gates, as the external stimuli can be described as inputs, and the relative position of the different molecular components can be regarded as outputs, in the frame of binary logic (0 and 1).[6] In this regard, a high selectivity of the macrocycle for the stations must be attained to precisely define the different states.

In principle, a processive[7] linear movement of the ring along the axle could be achieved upon increasing the number of stations. Nevertheless, while examples of two-station rotaxanes are common in the literature, inserting a higher number of different interaction sites on the axle is still challenging. Indeed, in order to obtain full control over the relative movements, a few requisites must be fulfilled: i) the ring must exhibit different affinity for different stations and the interaction should be selective, i.e., the ring should interact with only one station at a time, depending on the experimental conditions, to ensure the presence of only one of the possible co-conformational isomers; ii) the interactions between the ring and each station should be controllable by means of independent and orthogonal stimuli, so that each station can be switched on and off; iii) the reactions used for such switching processes should be reversible, to ensure repetitive operation (cycling). Moreover, in order to obtain a directionally controlled displacement of the ring, the stations should be positioned in a carefully designed sequence along the axle.

Three-station [2]rotaxanes are the logical evolution of molecular shuttles and represent the simplest platform to obtain processive linear motion.[8] Nevertheless, reports on such systems are very rare in the literature,

10.1002/anie.202414609

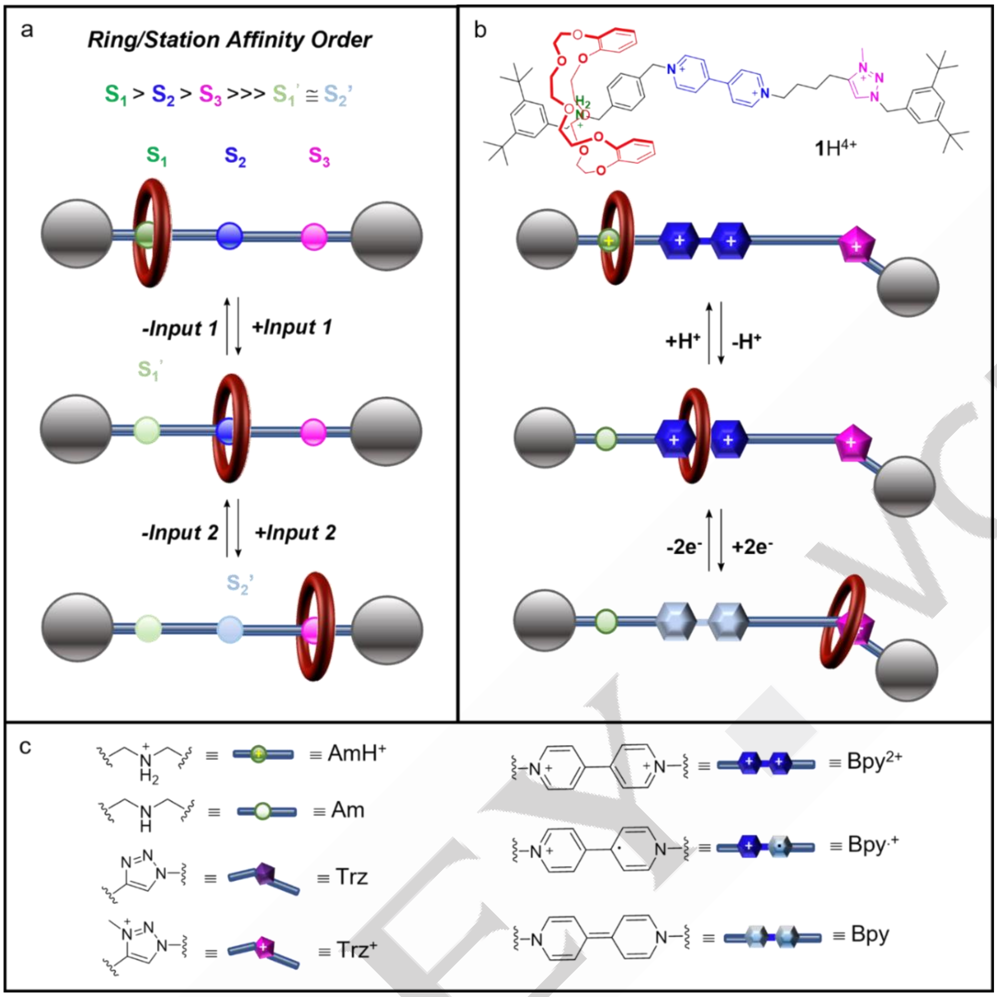

Figure 1. a) Design principle and operation mechanism of a directional three-station [2]rotaxane; b) molecular structure of [2]rotaxane **1**H^{4+} and its stimuli induced operation; c) cartoon representation of the main units of the [2]rotaxane axle and their abbreviation as used in the text.

and the requisites listed above are only seldom fulfilled.[9] In some cases, the macrocycle occupies selectively one of the three stations but its movement along the axle is not directional;[10] in other instances, once an external stimulus is applied, the ring shuttles between two recognition sites rather than translating,[11] and the inputs are neither independent nor selective.[12] In these systems, several co-conformational isomers are typically present for each state, with the consequence of hampering a precise control over the ring position.

Here we describe a novel [2]rotaxane in which the ring can perform two sequential translation steps along the same direction upon application of a sequence of two independent and orthogonal stimuli. The strength of the non-covalent interactions of the ring with either station on the axle, the clean and reversible character of the switching processes, and the overall unsophisticated structural design, render this system an efficient platform to develop artificial linear molecular motors.

Design

The design of three-station rotaxanes with the properties discussed above should include, therefore, three different interaction sites, two of which should be easily, orthogonally and reversibly switchable. Ideally, each switching reaction should turn off completely the recognition abilities of the respective station, to prevent an even distribution of the ring among different stations. In other words, to ensure a clean operation of the machine, one co-conformational isomer should be exclusively (or dominantly) populated in each state of the switching cycle. The three stations (S) incorporated in the axle component should possess the following features (Figure 1a): i) S1 (the primary station) should be the strongest interaction site for the ring; ii) S1 should be switched off completely as a station (to form S1') by a reversible reaction; iii) both S2 and S3 (the secondary and tertiary stations, respectively) should present an affinity for the ring lower than S1 and higher than S1'; iv) S2 should be a stronger station than S3; v) S2 should be switchable (to form S2') by a stimulus different and independent from that affecting S1; vi) the deactivated S2' should be a weaker station than S3.

With these guidelines in mind, we designed and synthetized the three-station [2]rotaxane **1**H^{4+} presented in Figure 1b. The macrocyclic component is dibenzo-24-crown-8 (DB24C8), a crown ether widely exploited for the construction of supramolecular and interlocked structures:[3,13] its electron-rich cavity and aromatic units enable the formation of hydrogen-bonding,[14] charge-transfer and π-π stacking interactions.[15] In the field of supramolecular chemistry, *sec*-ammonium (AmH^+) moieties are by far the strongest and most investigated sites of interaction for DB24C8, also exploited as templates to direct the synthesis of MIMs.[3]

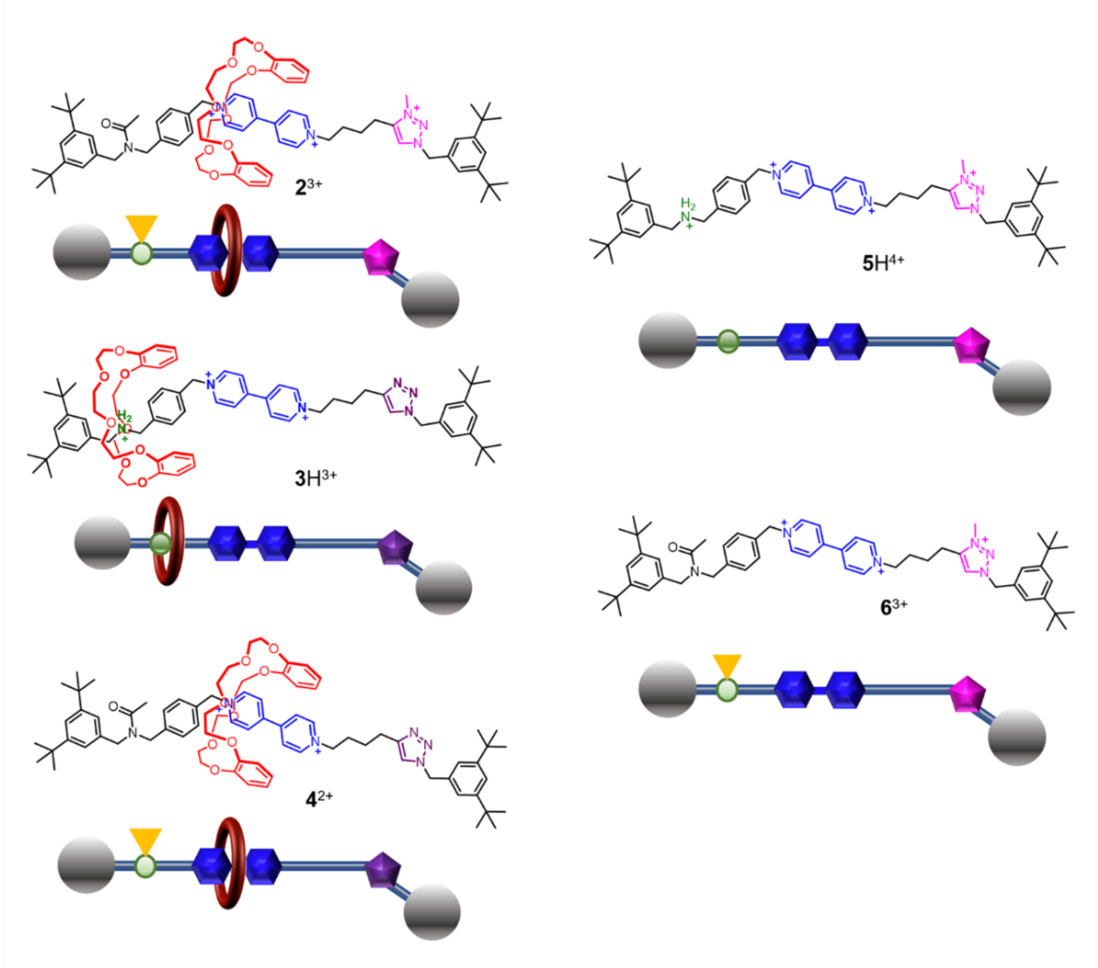

Figure 2. Structures of the model compounds and their cartoon representation.

Moreover, such recognition site can be completely switched off by deprotonation: the amine (Am) moiety, indeed, is a weak interaction site for DB24C8, and several units have been reported in the literature with a stronger affinity for the macrocycle.[16] Therefore AmH^+ was selected as station S1, as well as a templating group for the formation of the [2]rotaxane. Bipyridinium (Bpy^{2+}) is known to form complexes with aromatic crown ethers due to charge-transfer interactions, [15,17] which can be switched off by reduction of the bipyridinium ion through an electrochemical stimulus.[18] A Bpy^{2+} moiety was hence selected as secondary station S2, as the association constant values of its complexes with DB24C8 fall between those of AmH^+ and Am.[16a] Triazolium ions (Trz^+) interact very weakly with DB24C8 and have been reported as recognition sites in mechanically interlocked systems, generally in combination with *sec*-ammonium.[16b,19] It has been demonstrated that Trz^+ is a weaker station than AmH^+ (S1) but stronger than Am (S1')[19c] and, although no mechanically interlocked systems containing both Trz^+ and Bpy^{2+} have been previously characterized, data from the literature suggest that Trz^+ should be a weaker station than the bipyridinium (Bpy^{2+}, S2).[20] Moreover, Trz^+ is not affected by and does not interfere with any of the inputs used to deactivate S1 and S2. For these reasons, Trz^+ was chosen as tertiary station S3 of rotaxane **1**H^{4+}.

The postulated operation mechanism of the three-station rotaxane **1**H^{4+} is schematized in Figure 1b: in the initial state the ring encircles AmH^+ (S1); the deprotonation of AmH^+ (S1→S1') causes the ring translation toward the secondary station Bpy^{2+} (S2); upon electrochemical reduction of Bpy^{2+} to Bpy (S2→S2') the ring moves forward to interact with Trz^+ (S3). The system can be reset by oxidation of Bpy (S2'→S2) and protonation of Am (S1'→S1). To demonstrate and fully understand the processes driving the operation of **1**H^{4+}, a family of model compounds was synthetized (Figure 2). In rotaxane **2**$^{3+}$ the ammonium station is replaced by an inactive acetylated amine, in **3**H^{3+} the tertiary triazolium station is replaced by a triazole. As a matter of fact, compounds **2**$^{3+}$ and **3**H^{3+} are two-station [2]rotaxanes, i.e. molecular shuttles, which are triggered by electrochemical and acid-base inputs, respectively. Rotaxane **4**$^{2+}$ possesses only the bipyridinium interaction site. Finally, compounds **5**H^{4+} and **6**$^{3+}$ correspond to the axles of rotaxanes **1**H^{4+} and **2**$^{3+}$, respectively.

Results and Discussion

Synthesis

The synthesis of rotaxane **1**H^{4+} followed a stepwise modular approach starting from the preparation of alkyne functionalized pyridyl-pyridinium **7**$^+$ and the benzyl chloride derivative of the dibenzylammonium station **8**H^+. The microwave assisted SN_2 reaction between the two building blocks led to the formation of open thread **9**H^{3+}, characterized by the presence of a bulky 3,5-di-tert-butyl-benzyl group on one end, a moiety routinely used in DB24C8 incorporating rotaxanes as stopper, and presenting

10.1002/anie.202414609

two of the recognition sites of the target compound: dibenzylammonium (AmH$^+$) and bipyridinium (Bpy^{2+}). Although both of these stations have been reported to generate threaded complexes with DB24C8 in apolar solvents[3] mixing **9**H^{3+} with 1 equivalent of the crown ether in dichloromethane (DCM), allowed for the exclusive formation of the [2]pseudorotaxane in which the macrocycle resides on AmH$^+$. The corresponding [2]rotaxane **3**H^{3+} was obtained by stoppering the alkyne end of the complex by copper (I) catalyzed alkyne-azide click reaction (CuAAC) with 3,5-di-t-butylbenzylazide. The third recognition site of the system, triazolium (Trz$^+$) was generated by N-methylation with iodomethane of the triazole formed in the previous step. The final compound, **1**H^{4+}, was isolated as the hexafluorophosphate (PF_6^-) salt in good yield (Scheme 1). Deprotonation of compounds **1**H^{4+} and **3**H^{3+} followed by N-acetylation of the dibenzylamine group in neat acetic anhydride, afforded model compounds **2**$^{3+}$ and **4**$^{2+}$ respectively (Scheme S2). The successful construction of target [2]rotaxane **1**H^{4+} as well as reference compounds was confirmed by NMR spectroscopy and high resolution mass spectrometry (ESI section 1).

NMR characterization

Figure 3 shows the comparison between the ^{1}H NMR spectrum of compound **1**H^{4+} (Figure 3b) with the spectra of the free components DB24C8 (Figure 3a) and thread **5**H^{4+} (Figure 3c) in CD_2Cl_2. The signals were color coded to highlight their belonging or proximity to one of the three stations. The marked change in chemical shift of the protons signals associated with both the macrocycle and the axle, in particular those adjacent to AmH$^+$, confirm the formation of the interlocked structure, where the electron-rich cavity of DB24C8 interacts exclusively with AmH$^+$ through hydrogen bonding, as reported for analogous systems.[16a]

The reversible acid/base triggered translation of the macrocycle was initially investigated by ^{1}H NMR spectroscopy in CD_3CN as presented in Figure 4. In the initial state (Figure 4a) the crown ether encircles AmH$^+$. The addition of tributylamine (TBA, pKa= 18.09)[21] leads to the deprotonation of AmH$^+$, generating Am and lowering the association with the macrocycle, which then moves to the next available station, Bpy^{2+}(Figure 4b). In line with previous results,[16a] the translation of DB24C8 from Am onto Bpy^{2+} is reflected in the ^{1}H NMR spectrum as a drastic change in chemical shift of the protons related to these stations. In particular, the disappearance of the multiplet at 4.7 ppm, associated to the -C***H$_2$***-N-C***H$_2$***- protons in the complex, converted into two singlets at 3.8 ppm, shows that the amine is no longer encircled by the macrocycle. Moreover, the set of doublets (8.5 – 9 ppm) corresponding to the protons of Bpy^{2+} shifts significantly, confirming the interaction with the DB24C8 cavity. As a comparison, the spectrum of compound **2**$^{3+}$, in which the acetylation of Am forces the crown ether to reside onto Bpy^{2+}, is reported (Figure 4d). This spectrum shows an almost perfect match between the chemical shift of the Bpy^{2+} protons with those of the deprotonated [2]rotaxane **1**H^{4+}. The addition of trifluoroacetic acid (TFA, pKa= 12.65)[22] regenerates AmH$^+$, restoring the system to the initial state (Figure 4c). Interestingly, when AmH$^+$ is deactivated in CD_3CN, either by deprotonation or acetylation, with consequent translation of the macrocycle to the secondary station, the ^{1}H NMR spectra show a slight high field shift of the signals related to the Trz$^+$ protons, not detected when working in CD_2Cl_2 (Figure S29), suggesting that in these conditions the crown ether might be interacting with Trz$^+$. It is well known that in

Scheme 1. Synthesis of [2]rotaxane **1**H^{4+}.

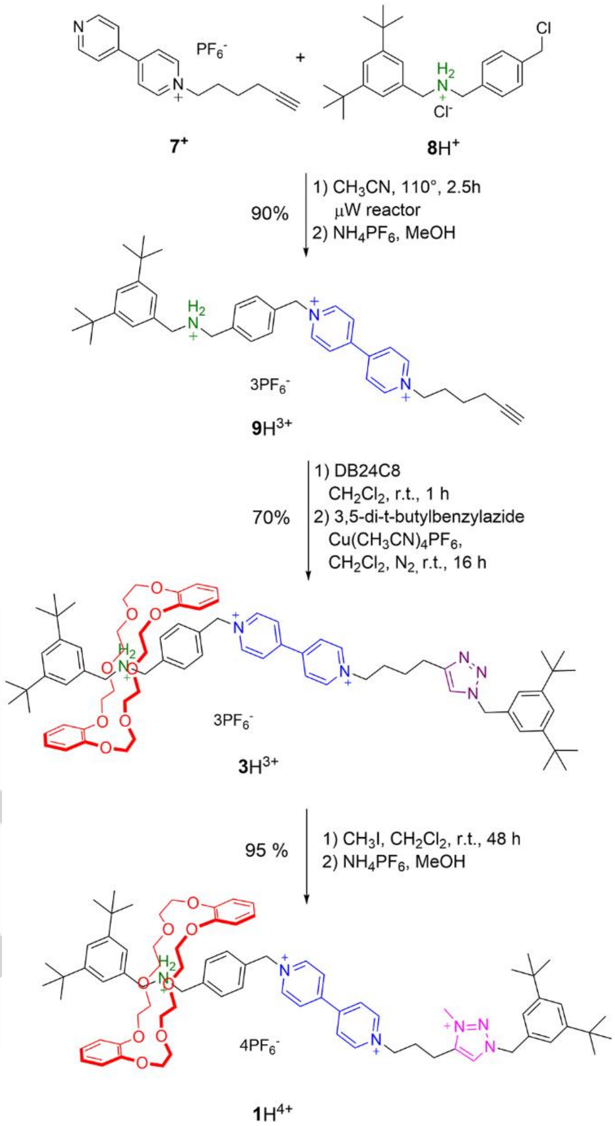

rotaxanes where Trz$^+$ acts as recognition site for DB24C8 and it is located within its cavity, the protons of the station are strongly de-shielded.[16,19] Here, it might be hypothesized that while the electron-rich cavity of DB24C8 surrounds Bpy^{2+}, it may adopt a chair conformation in which one of its aromatic groups sits partially over Trz$^+$, hence shielding its protons (ESI Section 4).

The movement of crown ether to Trz$^+$ upon deactivation of Bpy^{2+}, was monitored by ^{1}H NMR performing the reduction to the neutral Bpy species chemically, using cobaltocene as the reductant ($CoCp_2$, E = -0.94 V vs. SCE).[23] To prevent detrimental side reactions of the free amine of **1**$^{3+}$ with radical species, we decided to perform the experiment using model compound **2**$^{3+}$. Figure 4e shows the marked shifts of all the ^{1}H NMR signals associated with the protons of Trz$^+$ and neighboring groups when Bpy^{2+} is reduced using 10 equivalents of $CoCp_2$.[24] In particular, the singlet of the triazolium proton, at 8 ppm in **2**$^{3+}$, undergoes a shift to lower fields by 1 ppm in **2**$^+$, a clear confirmation that Trz$^+$ is located within the macrocycle cavity.[16,19] Moreover, the ROESY (Figure S35f) presents cross peaks between the signals of Trz$^+$ and DB24C8, confirming that, upon reduction of Bpy^{2+}, the macrocycle moves to the last station available, Trz$^+$.

10.1002/anie.202414609

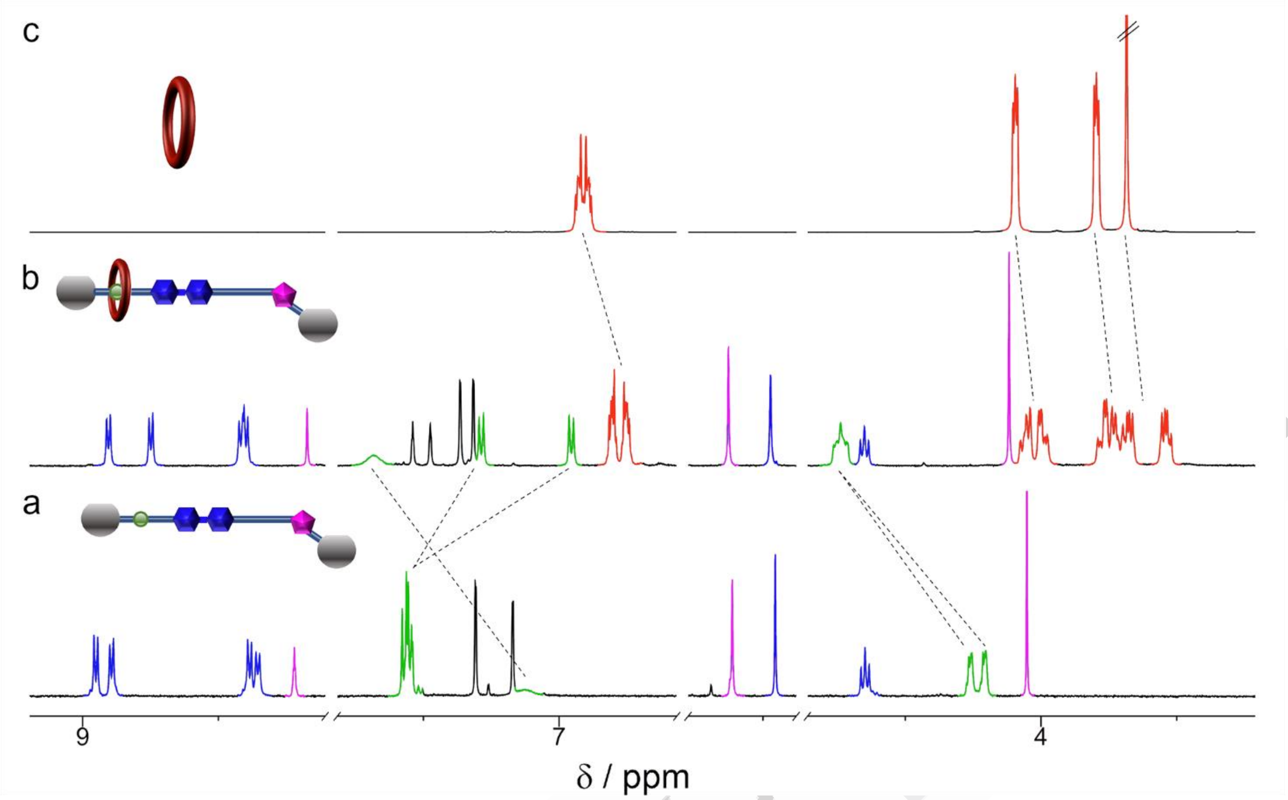

Figure 3. ^{1}H NMR spectra (500 MHz, CD_2Cl_2, 298 K) of a) axle **5**H^{4+}, b) [2]rotaxane **1**H^{4+} and c) DB24C8; color coding of the signals indicates: DB24C8 – red; AmH^+ - green; Bpy^{2+} - blue; Trz^+ - pink.

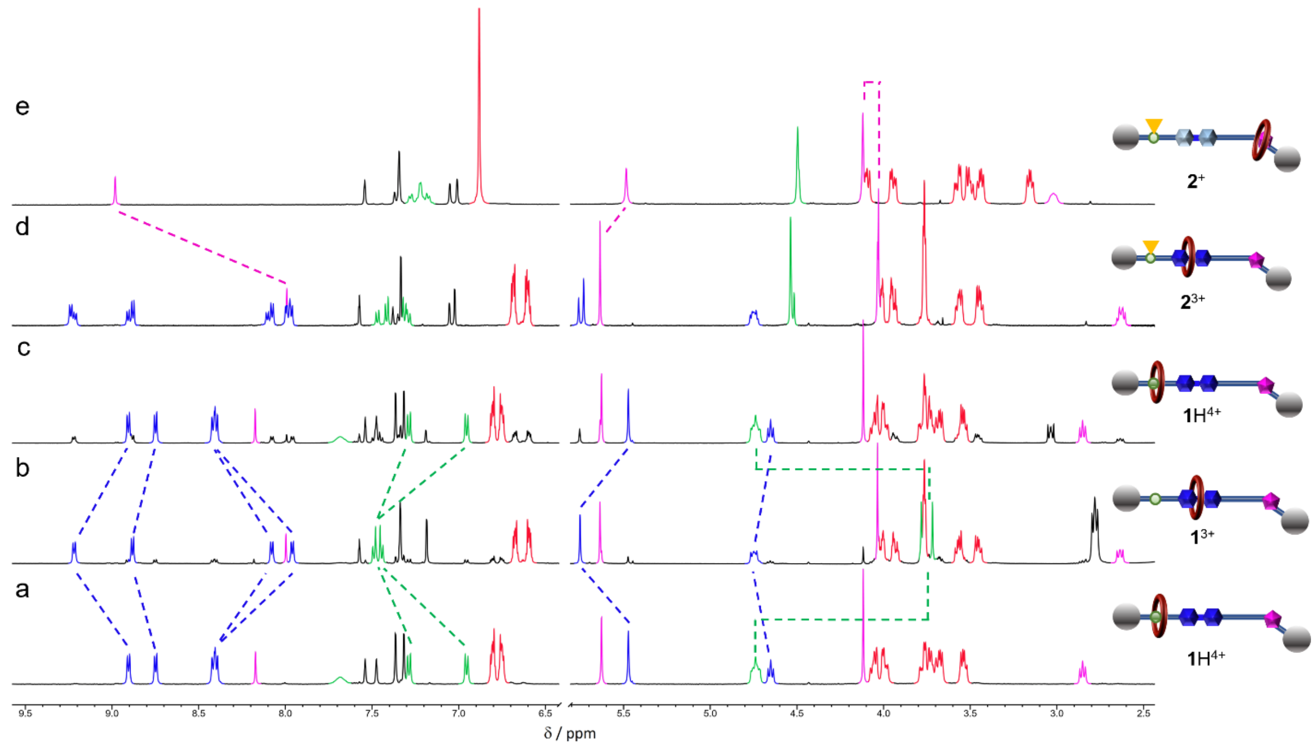

Figure 4. ^{1}H NMR spectra (500 MHz, CD_3CN, 298 K) of a) **1**H^{4+} 5 mM; b) sample (a) after the addition of TBA (~1 eq); c) sample (b) after the addition of TFA (~1 eq); d) **2**$^{3+}$ (5 mM); e) **2**$^{3+}$ (1 mM) after the addition of 10 eq of $CoCp_2$. Color coding of the signals indicates: DB24C8 – red; AmH^+ - green; Bpy^{2+} - blue; Trz^+ - pink.

10.1002/anie.202414609
WILEY-VCH

Electrochemical characterization

The operation of the rotaxanes via chemical and electrochemical stimuli was investigated by means of voltammetric experiments. Indeed, the synthetized compounds are characterized by the presence of two electroactive moieties, the Bpy^{2+} and the Trz^{+}. The Bpy^{2+} unit exhibits two monoelectronic and reversible reduction processes,[25] which are influenced by the presence of an electron donor host like DB24C8;[16a, 26] on its turn, the oxidation state of Bpy^{2+} affects its affinity for the macrocycle:[17,27] indeed, electrochemical reduction of the bipyridinium weakens the charge-transfer interaction with the crown ether.[18] The tertiary station Trz^{+} is characterized by a poorly reversible reduction process[28] which, in turn, can be affected by the interaction with the crown ether (vide infra). As a consequence, electrochemical inputs, besides modulating the secondary station affinity for the macrocycle, can give insight on its position along the axle. The electrochemical properties were investigated by cyclic voltammetry (CV) and differential pulse voltammetry (DPV) in CH_3CN and CH_2Cl_2: these two solvents have different coordination abilities, which influence the strength of the interactions between the crown ether and the stations. As the switching behavior of the rotaxanes in the two solvents is similar, only the experiments performed in CH_3CN will be discussed (see ESI section 6 for details about the electrochemical characterization). Reference compounds were studied to assess the electrochemical behavior of the free and complexed stations.

Axle compounds **5**H^{4+} and **6**$^{3+}$ are model molecules for the free electroactive units, as they contain free Bpy^{2+} and Trz^{+} together with AmH^{+} or the acetylated amine, respectively. Compounds **5**H^{4+}, **5**$^{3+}$ and **6**$^{3+}$ show a similar electrochemical behavior (Table 1), regardless of the state of the amine unit (protonated, deprotonated, or acetylated): two reversible monoelectronic reduction processes, which are ascribed to the first and second reduction of the Bpy^{2+},[26] and a poorly reversible process, at more negative potential values, which is attributed to the reduction of the Trz^{+} unit (Figure 5).[28]

Compound **4**$^{2+}$ is the model compound for the complexed secondary station, as AmH^{+} (S1) and Trz^{+} (S3) are both inactivated, and DB24C8 can only reside on Bpy^{2+} (S2). Bpy^{2+} is the only electroactive site in this molecule, and it undergoes two monoelectronic reduction processes both at more negative potential values compared to the free Bpy^{2+} in compounds **5**H^{4+} and **6**$^{3+}$ (Table 1 and Figure 5). Indeed, in the absence of secondary interaction sites, DB24C8 stabilizes both Bpy^{2+} and its monoreduced radical cation. We cannot exclude, though, that after the second electronic reduction the ring moves away from Bpy^{2+}, either randomly shuttling along the axle, oscillating between the fully reduced Bpy and the triazole, or moving toward the triazole unit.

Table 1. Reduction potential values (V vs SCE) of the examined compounds in CH_3CN.

Compound	$E^{1}_{1/2}$ [a]	$E^{2}_{1/2}$ [a]	E^{3}_{p} [b]
1H^{4+}	-0.35	-0.77	-1.70
1^{3+}	-0.51	-0.83	-1.92
2^{3+}	-0.50	-0.83	-1.91
3H^{3+}	-0.36	-0.79	/
3^{2+}	-0.56	-1.00	/
4^{2+}	-0.55	-1.01	/
5H^{4+}	-0.36	-0.78	-1.71
5^{3+}	-0.36	-0.79	-1.72
6^{3+}	-0.35	-0.79	-1.73

[a]Half-wave potential of the reversible processes, taken from cyclic voltammetries; [b]peak potential of the poorly reversible process, taken from differential pulse voltammetries.

Compound **3**H^{3+} is a two-station, chemically-driven rotaxane, which is a model for the acid-base driven shuttling between the primary and secondary stations. In analogy with related molecular shuttles,[26] two monoelectronic and reversible reduction processes are observed at similar potential values to those of the free axle compounds (Table 1); upon deprotonation of the ammonium site with the strong phosphazene base P_1, both processes are shifted to more negative potential values: indeed, deprotonation inactivates the former primary site, and the molecule behaves as the one-station rotaxane **4**$^{2+}$. Therefore these experiments confirm that DB24C8 resides exclusively on AmH^{+} (S1) and upon deprotonation (S1→S1') the ring shuttles to Bpy^{2+} (S2).

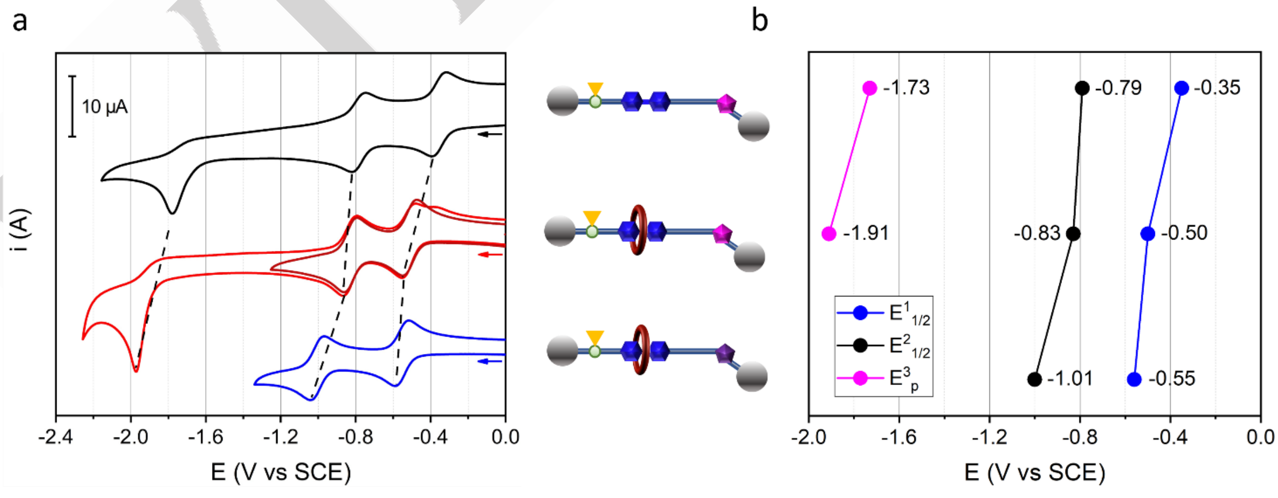

Figure 5. a) Cyclic voltammograms (scan rate: 100 mV s^{-1}) of a solution of **6**$^{3+}$ (3.4 × 10^{-4} M, black line), of **2**$^{3+}$ (3.5 × 10^{-4} M, red lines), and of **4**$^{2+}$ (3.5 × 10^{-4} M, blue lines). As the reduction of Trz^{+} causes the appearance of a new peak in the anodic scan (ESI section 6.1), another voltammetry, in which the scan is reversed before the reduction of the triazolium, is reported in the graph. Experimental conditions: argon-purged CH_3CN, room temperature, 100 equivalents of $TEAPF_6$. b) Genetic diagram of the half-wave and peak potentials of the acetylated rotaxane **2**$^{3+}$ compared with model axle **6**$^{3+}$ and model rotaxane **4**$^{2+}$.

10.1002/anie.202414609

Rotaxane **2**$^{3+}$ is an electrochemically-driven molecular shuttle, which is a model for the redox-driven shuttling between the secondary and tertiary stations. As a matter of fact, this is the first example of a rotaxane based on the Bpy^{2+}-Trz^{+} recognition sites couple. Three reduction processes can be observed in CH_3CN (Table 1 and Figure 5), which were interpreted as follows. Initially the macrocycle resides on Bpy^{2+}, as demonstrated by the first electrochemical reduction, which is at similar potential values as the first reversible reduction of the one-station rotaxane **4**$^{2+}$. The second reversible reduction process is only marginally shifted to negative values compared to the one of the free dumbbell, revealing a smaller influence of the ring on the $Bpy^{\cdot+}$ station after its first reduction. The last reduction process is poorly reversible, and it is at more negative potential values compared to the free Trz^{+} in the uncomplexed axle: therefore, this process was assigned to the reduction of Trz^{+} encircled by DB24C8. Overall, these results suggest that, in a molecular shuttle based on a Bpy^{2+}-Trz^{+} couple: i) the primary station for DB24C8 is Bpy^{2+}, as revealed by ^{1}H NMR spectra (i.e., S2 is a better station than S3); ii) the reduction of Bpy^{2+} lowers the affinity of the crown ether for this station (S2→S2'); iii) after the second reduction of Bpy^{2+}, DB24C8 moves towards Trz^{+}, which is therefore a better recognition site than the bi-reduced Bpy, as evidenced by ^{1}H NMR spectra (i.e., S3 is a better station than S2'). To further understand the switching mechanism of rotaxane **2**$^{3+}$, the cyclic voltammograms were fitted according to the mechanism reported in Scheme 2 (see ESI section 6.2 for details), in order to evaluate the ring population distribution between the two stations at different redox states. In CH_3CN, the rings surround Bpy^{2+} in the initial state (K_1= 5 x 10^{-4}) and, after the first reduction, around 25% of the rings moves away (K_2= 0.33), due to the weaker charge-transfer interaction. The full translocation of the rings is achieved after the second reduction (K_3= 1700), which completely switches off the bipyridinium station. A similar pattern is observed in CH_2Cl_2 (K_1= 3 x 10^{-4}, K_2= 3.2, K_3= 25000) with the difference that around 70% of the rings moves to Trz^{+} already upon the first reduction of Bpy^{2+}, making the switching process more efficient. The fatigue resistance of **2**$^{3+}$ to electrochemical switching was investigated inducing multiple sequential reduction and re-oxidation processes of Bpy^{2+}. This experiment was performed repeating CVs without renewing the diffusion layer and therefore addressing the same ensemble of molecules (Figure S41). The repetition of the switching up to 10 times did not lead to any significant change in the voltammetric curves, proving the high degree of reversibility of the process.

Finally, the electrochemical behavior of rotaxane **1**H^{4+} can be interpreted considering the information gathered from reference compounds. The voltammetries of **1**H^{4+} in CH_3CN show four reduction processes (Figure 6): the first two can be safely assigned, by comparison with axles **5**H^{4+} or **6**$^{3+}$, to the first (-0.35 V vs SCE) and second (-0.77 V vs SCE) reduction of the free Bpy^{2+}. The other two poorly reversible processes occur at -1.70 and -1.92 V vs SCE, which correspond to the reduction of free and complexed Trz^{+}, respectively, as it can be inferred by comparison with axle **6**$^{3+}$ and rotaxane **2**$^{3+}$. Such observation is assigned to a deprotonation process triggered by the reduction of the free Trz^{+}. In presence of acid, the reduced triazolium uptakes a proton: as the source of protons is the rotaxane **1**H^{4+} itself, deprotonation of AmH^{+} and shuttling of DB24C8 should occur, leading to the process at -1.92 V vs SCE (ESI page 49). It must be emphasized, though, that this process does not interfere with the operation of the rotaxane: indeed, reduction of Trz^{+} enables to read the state of the system, but is not necessary for the operation of the molecular machine. Overall, the electrochemical behavior of rotaxane **1**H^{4+} is reminiscent of the axle models, meaning that DB24C8 ring surrounds AmH^{+} and does not interact with Bpy^{2+}.

Scheme 2. Scheme related to the co-conformational equilibria of **2**$^{3+}$ for the different redox states of the bipyridinium unit. The vertical processes represent the redox reactions of Bpy^{2+}, while the horizontal processes represent the shuttling of DB24C8 from Bpy^{2+} to Trz^{+} (the relative populations for each redox state are reported). Counterions are omitted for clarity.

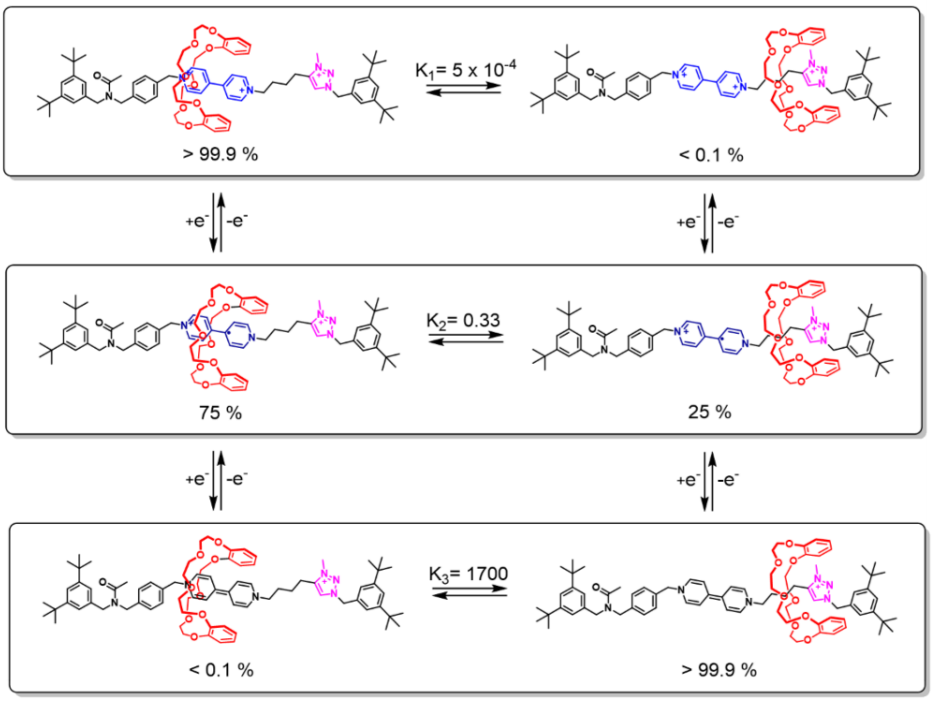

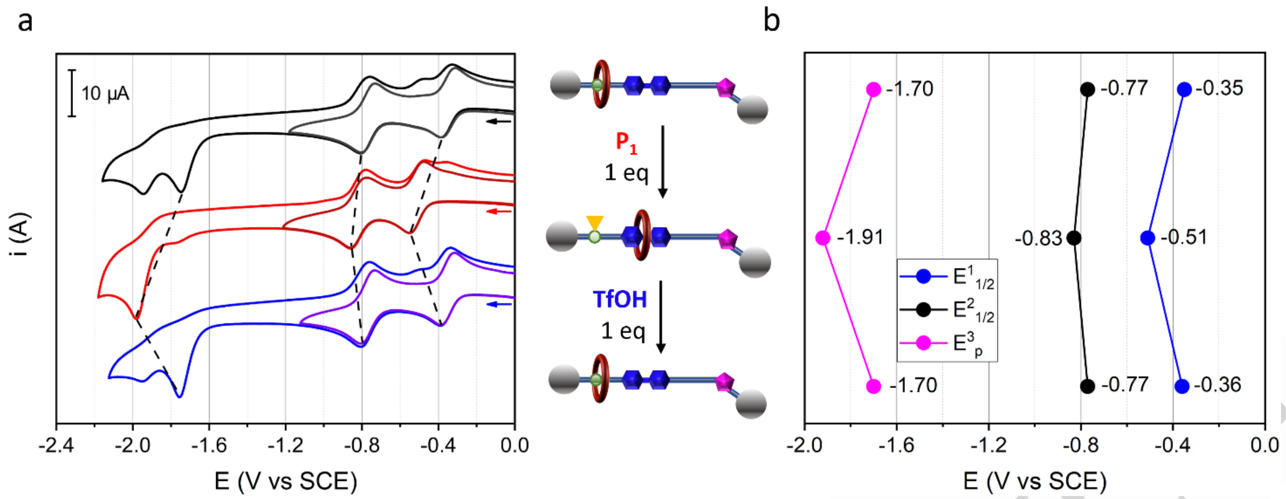

Figure 6. a) Cyclic voltammograms (scan rate: 200 mV s^{-1}) of a solution of **1**H^{4+} (4.0 × 10^{-4} M, black and gray lines), and of the same solution upon sequential addition of 1 equivalent of P_1 base (red lines) and 1 equivalent of triflic acid (blue lines). As the reduction of Trz$^+$ causes the appearance of new peaks in the anodic scan, other voltammetries, in which the scan is reversed before the reduction of the triazolium, are reported in the graph. Experimental conditions: argon-purged CH_3CN, room temperature, 100 equivalents of $TEAPF_6$. b) Genetic diagram of the half-wave and peak potentials of the protonated rotaxane **1**H^{4+} upon addition of 1 equivalent of P_1 base and 1 equivalent of triflic acid.

Upon deprotonation of rotaxane **1**H^{4+} with P_1 base (pKa= 26.88),[29] the first reduction of Bpy^{2+} is shifted to more negative values (-0.50 V vs SCE), whereas the reduction of the free Trz$^+$ disappears (Figure 6). The electrochemical behavior of **1**$^{3+}$ is analogous to the one of the two-station rotaxane **2**$^{3+}$, in which the macrocycle initially surrounds Bpy^{2+} and moves onto Trz$^+$ when Bpy^{2+} is bi-reduced. The subsequent addition of triflic acid (pKa= 0.70),[30] to a solution of **1**$^{3+}$ restores the voltammograms of **1**H^{4+} (Figure 6), proving the reversibility of the deprotonation process, in agreement with NMR experiments.

The operation of [2]rotaxane **1**H^{4+} can be summed up as follows: i) on the protonated rotaxane, DB24C8 resides on AmH$^+$, the primary station; ii) after deprotonation, the primary station is deactivated, and the macrocycle moves towards Bpy^{2+}, the secondary station; iii) upon electrochemical reduction, Bpy^{2+} is deactivated and the crown ether moves towards the Trz$^+$, the tertiary station. The reversibility of the redox and acid-base processes of the bipyridinium and of the Am/AmH$^+$ couple allows to reset the system to the initial state. Overall, a processive motion of the ring is obtained, by means of consecutive, orthogonal and reversible stimuli.

Thermodynamic considerations

The controlled motion of the macrocycle along the axle in **1**H^{4+} is achieved modulating the affinity of the crown ether for the different stations through chemical and electrochemical stimuli. The thermodynamics of the system can be evaluated using the electrochemical data (*vide supra*) and the pK_a of model compounds, determined in CH_3CN by ^{1}H NMR spectroscopy titrations (ESI section 7.2). Indeed, considering the square scheme reported in Scheme 3, it is possible to express the equilibrium constant K_4 as:

$$K_4 = \frac{K_a^{app} - K_a}{K_a' - K_a^{app}}$$

where K_a^{app} is the apparent acidity constant of rotaxane **3**H^{3+}, K_a is the acidity constant of AmH$^+$ surrounded by the macrocycle and K_a' the one of the free AmH$^+$ (see ESI section 7.1 for derivation of the equation and details). In CH_3CN, K_a^{app} and K_a' were determined to be 6.3 x 10^{-18} M and 6.3 x 10^{-16} M respectively, by titration of rotaxane and axle model compounds (ESI section 7.2), while K_a can be estimated, according to literature,[31] to be around 5 x 10^{-27}.

Scheme 3. Scheme related to the co-conformational equilibria of **3**H^{3+} for the different states of the ammonium station. The vertical processes represent deprotonation of AmH$^+$, while the horizontal processes represent the shuttling of DB24C8 from AmH$^+$ to Bpy^{2+} (the relative populations for each state are reported). Counterions are omitted for clarity.

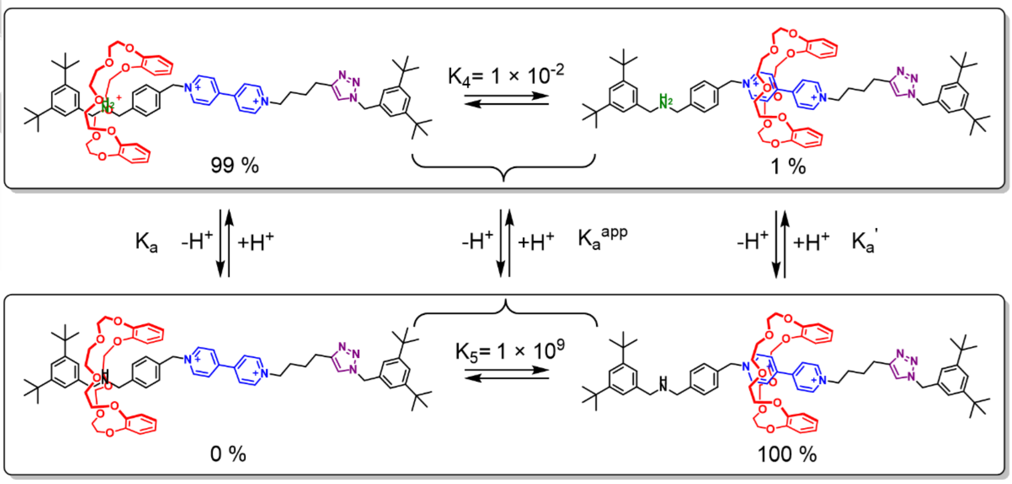

10.1002/anie.202414609

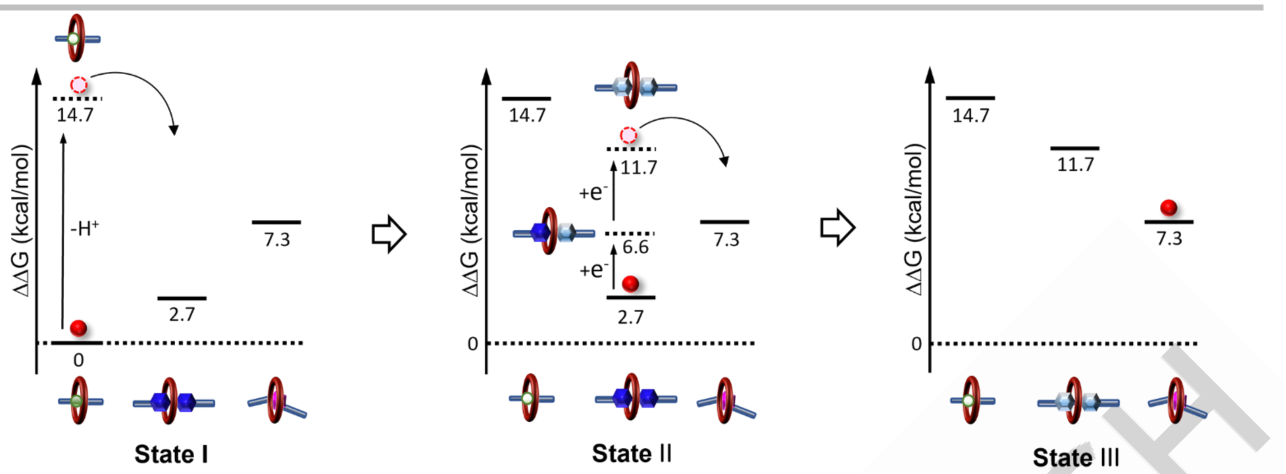

Figure 7. Energetic diagrams related to the interaction of the macrocycle with the different stations of rotaxane **1**H^{4+} in CH_3CN at 298 K when no stimulus is applied (State I), upon deprotonation of the ammonium station (State II) and upon subsequent reduction of the bipyridinium station (State III).

Combining the equilibrium constants obtained from the pK_a with the redox potentials obtained from the fitting of the CV curves allows to define the relative arrangement of the energy levels related to the interaction of the macrocycle with different stations in CH_3CN (Figure 6, ESI section 7.3). When no stimulus is applied (State I), the energy difference between AmH^+ and Bpy^{2+} amounts to 2.7 kcal/mol and 99% of the rings is located on the primary station. When the ammonium station is switched off by deprotonation (State II), the energy of the state corresponding to Am encircled by DB24C8 rises by over 14 kcal/mol and the ring moves towards Bpy^{2+}. Upon mono- and bi-reduction of Bpy^{2+}, the energy rises by 6.6 and 11.7 Kcal/mol, respectively. Overall, when Bpy^{2+} is doubly reduced, the energy level corresponding to the interaction of DB24C8 with the fully reduced Bpy rises to 4.4 kcal/mol over the one corresponding to the interaction with Trz^+, leading to the movement of the ring on the third station (State III). Overall, the relative position of these energy levels allows rotaxane **1**H^{4+} to be switched quantitatively from State I to State II by addition of base and from State II to State III by electrochemical reduction; then the return to State II and State I can be obtained applying a reverse sequence of stimuli (re-oxidation of Bpy^{2+} followed by protonation of Am), due to the reversibility of the processes.

Conclusion

We reported the design, synthesis and characterization of a directional tristable [2]rotaxane, in which the linear motion of the macrocycle along the axle can be controlled by means of orthogonal and reversible chemical and electrochemical inputs. Indeed, the [2]rotaxane exhibits the following properties: i) the activation and deactivation reactions are orthogonal and reversible; ii) the position of the macrocycle on the axle is highly selective for each of the three stations; iii) the shuttling of the macrocycle along the axle component is directionally controlled, i.e. a processive linear motion is obtained; iv) the large affinity difference of the ring towards the stations in the different states makes the switching process robust. To the best of our knowledge, this is the first example of a tristable rotaxane that incorporates such properties, which are fundamental requisites for the realization of processive linear motion in such multifunctional rotaxane architectures. One important feature that characterizes this system is its modularity: indeed, investigation of model molecules indicates that each module of the system behaves almost independently from the others, thus enabling a great deal of planning ability. In principle, by a proper design, which should take into account also the kinetics of the shuttling motions, oligomers or polymers could be constructed based on these molecular modules.

Supporting Information

The authors have cited additional references within the Supporting Information.[32]

Acknowledgements

Financial support from the European Union's Horizon 2020 research and innovation program (FET-OPEN “Magnify” 801378) is gratefully acknowledged.

Keywords: Molecular Machines • Rotaxanes • Crown ethers • Bypiridinium • Ammonium • Triazolium

10.1002/anie.202414609

Entry for the Table of Contents

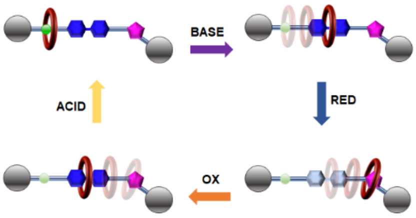

A [2]rotaxane comprising a dibenzo-24-crown-8 macrocycle and a thread containing three recognition sites (ammonium, bipyridinium and triazolium) is described. The ammonium and bipyridinium stations are responsive to orthogonal stimuli, pH and electrochemical, allowing control over the macrocycle movement along the axle. The thermodynamic characterization elucidated the processes driving the operation.

[1] M. Xue, Y. Yang, X. Chi, X. Yan, F. Huang, *Chem. Rev.* **2015**, *115*, 7398–7501.

[2] a) S. Erbas-Cakmak, D. A. Leigh, C. T. McTernan, A. L. Nussbaumer, *Chem. Rev.* **2015**, *115*, 10081–10206; b) M. Baroncini, S. Silvi, A. Credi, *Chem. Rev.* **2020**, *120*, 200–268.

[3] C. J. Bruns, J. F. Stoddart, The Nature of the Mechanical Bond: From Molecules to Machines; John Wiley and Sons, **2016**.

[4] H. Y. Zhou, Q. S. Zong, Y. Han, C. F. Chen, *Chem. Commun.* **2020**, *56*, 9916–9936.

[5] B. Yao, H. Sun, L. Yang, S. Wang, X. Liu, *Front. Chem.* **2020**, *9*, 832735.

[6] F. Nicoli, E. Paltrinieri, M. Tranfic Bakic, M. Baroncini, S. Silvi, A. Credi, *Coord. Chem. Rev.* **2021**, *428*, 213589.

[7] In processive motors the motor molecule moves along the track without losing contact, a condition ensured by the mechanical bond in interlocked molecules.

[8] D. D. Hackney, *Nature* **1995**, *377*, 448–450.

[9] a) G. Bottari, F. Dehez, D. A. Leigh, P. J. Nash, E. M. Pérez, J. K. Wong, F. Zerbetto, *Angew. Chem. Int. Ed.* **2003**, *42,* 5886–5889*;* b) A. Carlone, S. M. Goldup, N. Lebrasseur, D. A. Leigh, A. Wilson, *J. Am. Chem. Soc.* **2012**, *134*, 8321 - 8323; c) Z. Meng, C. F. Chen, *Org. Biomol. Chem.* **2014**, *12*, 6937–6943.

[10] a) A. C. Fahrenbach, Z. Zhu, D. Cao, W.-G. Liu, H. Li, S. K. Dey, S. Basu, A. Trabolsi, Y. Y. Botros, W. A. Goddard III, J. F. Stoddart, *J. Am. Chem. Soc.* **2012**, *134*, 16275 – 16288; b) L. Liu, Y. Liu, P. Liu, J. Wu, Y. Guan, X. Hu, C. Lin, Y. Yang, X. Sun, J. Ma, L. Wang, *Chem. Sci.* **2013**, *4*, 1701 – 1706; c) Y.-C. You, M.-C., Tzeng, C.-C. Lai, S.-H. Chiu, *Org. Lett.* **2012**, *14*, 1046 – 1049.

[11] a) W. K. Wang, Z. Y. Xu, Y. C. Zhang, H. Wang, D. W. Zhang, Y. Liu, Z. T. Li, *Chem. Commun.* **2016**, *52*, 7490-7493; b) Y. Wang, T. Cheng, J. Sun, Z. Liu, M. Frasconi, W. A. Goddard III, J. F. Stoddart, *J. Am. Chem. Soc.* **2018**, *140* , 13827–13834; c) E. Busseron, C. Romuald, F. Coutrot, *Chem. Eur. J.* **2010**, *16*, 10062 -10073; d) P. Waeles, K. Furnel-Marotte, F. Coutrot, *Chem. Eur. J.* **2017**, *23*, 11529 – 11539.

[12] a) T. Ikeda, S. Saha, I. Aprahamian, K. C.-F. Leung, A. Williams, W.-Q. Deng, A. H. Flood, W. A. Goddard III, J. F. Stoddart, *Chem. Asian. J.* **2007**, *2*, 76 – 93; b) M. Kimura, T. Mizuno, M. Ueda, S. Miyagawa, T. Kawasaki, Y. Tokunaga, *Chem. Asian J.* **2017**, *12*, 1381 – 1390.

[13] F. Nicoli, M. Baroncini, S. Silvi, J. Groppi, A. Credi, *Org. Chem. Front.* **2021**, *8*, 5531-5549.

[14] P. R. Ashton, E. J. T. Chrystal, P. T. Glink, S. Menzer, C. Schiavo, N. Spencer, J. F. Stoddart, P. A. Tasker, A. J. P. White, D. J. Williams, *Chem. Eur. J.* **1996**, *2*, 709 – 728.

[15] T. Gasa, J. M. Spruell, W. R. Dichtel, T. J. Sorensen, D. Philp, J. F. Stoddart, P. Kuzmic, *Chem. Eur. J.* **2009**, *15*, 106–116.

[16] a) P. R. Ashton, R. Ballardini, V. Balzani, I. Baxter, A. Credi, M. C. T. Fyfe, M. T. Gandolfi, M. Gómez-López, M.-V. Martínez-Díaz, A. Piersanti, N. Spencer, J. F. Stoddart, M. Venturi, A. J. P. White, D. J. Williams, *J. Am. Chem. Soc.* **1998**, *120* (46), 11932-11942; b) F. Coutrot, *ChemistryOpen* **2015**, *4*, 556–576; c) B. Riss-Yaw, J. Morin, C. Clavel, F. Coutrot, *Molecules* **2017**, *22*, 2017.

[17] P. L. Anelli, P. R. Ashton, R. Ballardini, V. Balzani, M. Delgado, M. T. Gandolfi, T. T. Goodnow, A. E. Kaifer, D. Philp, M. Pietraszkiewicz, L. Prodi, M. V. Reddington, A. M. Z. Slawin, N. Spencer, J. F. Stoddart, C. Vicent, D. J. Williams, *J. Am. Chem. Soc.* **1992**, *114*, 193–218.

[18] P. R. Ashton, R. Ballardini, V. Balzani, A. Credi, K. R. Dress, E. Ishow, C. J. Kleverlaan, O. Kocian, J. A. Preece, N. Spencer, J. F. Stoddart, M. Venturi, *Chem. Eur. J.* **2000**, *6*, 2558 -3574.

[19] a) G. Ragazzon, A. Credi, B. Colasson, *Chem. Eur. J.* **2017**, *23*, 2149; b) F. Coutrot, E. Busseron, *Chem. Eur. J.* **2008**, *14*, 4784-4787; c) F. Coutrot, C. Romuald, E. Busseron, *Org. Lett.* **2008**, *10*, 3741–3744.

[20] As DB24C8 interacts with Bpy^{2+} and Trz^{+} through charge-transfer interactions, the relative affinity for the two stations is related to the extent of their electron-poor character, which can be estimated from their reduction potentials (around -0.4[26] and -1.6[28] V vs SCE in CH_3CN, respectively). Therefore, as Bpy^{2+} is more electron-poor than Trz^{+}, it is expected to be a better station for the ring. This aspect will be experimentally proven in this study.

[21] J. F. Coetzee, G. R. Padmanabhan, *J. Am. Chem. Soc.* **1965** *87* (22), 5005-5010.

[22] J . T. Muckerman, J. H. Skone, M. Ning, Y. Wasada-Tsutsui, *Biochim. Biophys. Acta - Bioenerg.* **2013**, *1827*, 8–9, 882-891.

[23] W. E. Geiger, *J. Am. Chem. Soc.* **1974** *96* (8), 2632-2634.

[24] The signals related to the protons of the neutral Bpy moiety are not present in the ^{1}H-NMR spectrum (Figure 4e), due to an electron self-exchange between the neutral Bpy and traces of the Bpy$^{(\cdot+)}$ radical cation (See reference [32] and ESI Section 5 for details).

[25] I. P. Krainov, S. F. Kramarenko, E. I. Dotsenko, A. A. Bumber, E. S. Klimov, O. Y. Okhlobystin, *Chem. Heterocycl. Compd.* **1986**, *22*, 513–516.

[26] G. Ragazzon, C. Schäfer, P. Franchi, S. Silvi, B. Colasson, M. Lucarini, A. Credi, *Proc. Natl. Acad. Sci. U.S.A.* **2018**, *115*, 9385–9390.

[27] P. R. Ashton, R. Ballardini, V. Balzani, E. C. Constable, A. Credi, O. Kocian, S. J. Langford, J. A. Preece, L. Prodi, E. R. Schofield, N. Spencer, J. F. Stoddart, S. Wenger, *Chem. Eur. J.* **1998**, *4*, 2413-2422.

[28] A. Rapakousiou, C. Mouche, M. Duttine, J. Ruiz, , D. Astruc, *Eur. J. Inorg. Chem.* **2012**, 5071–5077.

[29] R. Schwesinger, J. Willaredt, H. Schlemper, M. Keller, D. Schmitt, H. Fritz, *Chem. Ber.* **1994**, *127*, 2435.

[30] E. Raamat, K. Kaupmees, G. Ovsjannikov, A. Trummal, A. Kütt, J. Saame, I. Koppel, I. Kaljurand, L. Lipping, T. Rodima, V. Pihl, I. A. Koppel, I. J. Leito, *Phys. Org. Chem.* **2013**, *26*, 162−170.

[31] M. J. Power, D. T. J. Morris, I. J. Vitorica-Yrezabal, D. A. Leigh, *J. Am. Chem. Soc.* **2023**, 145, 15, 8593–8599.

[32] J. M. Bobbitt, N. A. Eddy, C. X. Cady, J. Jin, J. A. Gascon, S. Gelpí-Dominguez, J. Zakrzewski, M. D. Morton, *J. Org. Chem.* **2017**, *82*, 9279.